Dynamics of fluctuations and thermal buckling in graphene from a phase-field crystal model

Enzo Granato [1,2] K. R. Elder [3] S. C. Ying [2] and T. Ala-Nissila [4,2,5]

[1]*Instituto Nacional de Pesquisas Espaciais, 12227-010 São José dos Campos, SP, Brazil*

[2]*Department of Physics, P.O. Box 1843, Brown University, Providence, Rhode Island 02912-1843, USA*

[3]*Department of Physics, Oakland University, Rochester, Michigan 48309, USA*

[4]*QTF Centre of Excellence, Department of Applied Physics, Aalto University School of Science, P.O. Box 11000, FI-00076 Aalto, Espoo, Finland*

[5]*Interdisciplinary Centre for Mathematical Modelling, Department of Mathematical Sciences, Loughborough University, Loughborough, Leicestershire LE11 3TU, United Kingdom*

(Received 24 October 2022; revised 10 January 2023; accepted 17 January 2023; published 24 January 2023)

We study the effects of thermal fluctuations and pinned boundaries in graphene membranes by using a phase-field crystal model with out-of-plane deformations. For sufficiently long times, the linear diffusive behavior of height fluctuations in systems with free boundaries becomes a saturation regime, while at intermediate times the behavior is still subdiffusive as observed experimentally. Under compression, we find mirror buckling fluctuations where the average height changes from above to below the pinned boundaries, with the average time between fluctuations diverging below a critical temperature corresponding to a thermally induced buckling transition. Near the transition, we find a nonlinear height response in agreement with recent renormalization-group calculations and observed in experiments on graphene membranes under an external transverse force with clamped boundaries.

DOI: 10.1103/PhysRevB.107.035428

I. INTRODUCTION

Thermally induced fluctuations in atomically thin crystals, such as graphene, lead to striking effects on its mechanical properties that can be eventually manipulated for technological applications [1–5]. Out-of-plane deformations, for example, allow for a thermally rippled, but flat phase, observed experimentally in free-standing graphene [6–8], where the bending rigidity and elastic modulus are strongly dependent on the length scale [9,10]. They also influence the dynamics in a remarkable way, as shown in experiments on free-standing graphene with scanning tunneling microscopy [11], giving rise to an anomalous diffusive behavior of the height fluctuations and a non-Gaussian velocity distribution.

Very recently, the dynamical behavior of out-of-plane fluctuations of freestanding graphene [12] was studied by using a phase-field-crystal (PFC) model, which allows for out-of-plane deformations in addition to the in-plane deformations included in standard PFC models [13–15]. The model describes the system by two coupled continuous fields, representing the particle density and the out-of-plane fluctuations with a small amplitude. It was found that the dynamic scaling behavior [16] depends only on the equilibrium roughening exponent ξ and the height displacement fluctuations at intermediate times behaves as $\langle \Delta h(t)^2 \rangle \propto t^{\alpha}$ with $\alpha = \xi/(1+\xi)$. This is in good agreement with the anomalous diffusion exponent observed experimentally [11]. At sufficient long times, however, the behavior is the usual linear diffusion for systems with free boundaries. On the other hand, in many experimental conditions the boundaries may be clamped or pinned. Molecular-dynamics simulations of atomistic models of graphene under compression and fixed boundaries [11,17] have revealed large fluctuations corresponding to local curvature inversion of the height at the central region, or mirror-buckling fluctuations, at sufficient high temperatures and argued to be responsible for the anomalous diffusive behavior. However, the origin and the effects of such mirror-buckling fluctuations on the anomalous diffusive behavior are still not fully understood. The boundary confinement could also affect the anomalous diffusive behavior even in unstrained membranes by constraining the center-of-mass diffusion in the long-time limit. Under compression, it can induce elastic instabilities in the form of a buckling transition with the spatially averaged height $\bar{h}$ acting as an order parameter, which is strongly affected by thermal fluctuations [18,19]. The proximity to the buckling transition should also have important influences on the height response to an external force applied perpendicularly to the membrane [18], which can be accessed experimentally in graphene membranes with clamped boundaries under an applied electric field [5]. It is thus of interest to investigate the effects of pinned boundaries on the out-of-plane and mirror-buckling fluctuations.

In this work, we study the effects of thermal fluctuations in graphene membranes using the PFC model with out-of-plane deformations [12,20], extended to include the effects of pinned boundaries. It is found that at sufficiently long times, the linear diffusive behavior of height fluctuations in systems with free boundaries becomes a saturation regime, while at intermediate times the behavior is still subdiffusive as found experimentally [11]. Under compression,

we find mirror buckling fluctuations with the average time between fluctuations diverging below a thermally induced buckling transition. We also determine the height response to an external transverse force near this transition and find a nonlinear force-displacement relation $f \propto \langle \bar{h} \rangle^{\delta_{\rm eff}}$ for small forces. Above the transition, the exponent $\delta_{\rm eff}$ is consistent with $3 - 1/\beta$, where β is the order-parameter critical exponent, as predicted by a recent renormalization-group calculations [18] and also observed in experiments on graphene membranes with clamped boundaries [5].

II. PHASE-FIELD-CRYSTAL MODEL WITH OUT-OF-PLANE DEFORMATIONS AND BOUNDARY POTENTIAL

We use the PFC model with out-of-plane deformations introduced previously [12,20], here extended to include the effects of pinned boundaries. The model is described by the effective Hamiltonian

$$\frac{H}{c_{\rm g}} = \int d^2\vec{r}\Bigg[\left(\frac{\Delta B}{2}n^2 + \frac{B_x}{2}n(\nabla_s^2+1)^2 n + \frac{\tau}{3}n^3 + \frac{v}{4}n^4\right) + \frac{1}{2}\kappa \int d\vec{r}\,' C(\vec{r}-\vec{r}\,')h(\vec{r}\,)h(\vec{r}\,') + V_n(\vec{r}\,)n(\vec{r}\,) + \frac{1}{2}V_h(\vec{r}\,)h(\vec{r}\,)^2\Bigg], \tag{1}$$

where $n(\vec{r}\,)$ is density field, $h(\vec{r}\,)$ is the height displacement measured from a base plane with $\vec{r} = (x, y)$, and $c_{\rm g}$ is an energy-scale parameter. In Fourier space, $C(k) = k^4$ for $k < k_{\rm max}$ and $C(k) = C_{\rm max}$ for $k > k_{\rm max}$. Values of $C_{\rm max}$ and $k_{\rm max}$ are chosen to eliminate small scale fluctuations of $h(\vec{r}\,)$. The surface Laplacian is approximated by

$$\nabla_s^2 \approx \nabla_{xy}^2 - \left(h_x^2\partial_x^2 + h_y^2\partial_y^2 + 2h_x h_y \partial_x\partial_y\right), \tag{2}$$

where $h_x = \partial h/\partial x$ and $h_y = \partial h/\partial y$. The first four terms in Eq. (1) correspond to the standard PFC model, leading to periodic patterns of $n(\vec{r}\,)$, while the next term represents the bending energy of the membrane, controlled by the bending stiffness κ. The new last two terms favor $n(\vec{r}\,) = n_{\rm gs}(\vec{r}\,)$ and $h(\vec{r}\,) = 0$ near the boundaries of the system, when the boundary potentials $V_n(\vec{r}\,)$ and $V_h(\vec{r}\,)$ are chosen appropriately, where $n_{\rm gs}$ is the ground-state configuration in absence of these potentials. The introduction of a boundary potential is particularly convenient for the numerical simulations since it still allows the use of periodic boundary conditions. The values of the bulk parameters entering the model were chosen to represent graphene [20], with a honeycomb pattern of maxima in the density field $n(\vec{r}\,)$, corresponding to $\Delta B = -0.15$, $B_x = 1$, $\tau = 0.874\,818$, $v = 1$, $\kappa = 0.209\,726$ and $c_{\rm g} = 6.58\,{\rm eV}$.

The time evolution is obtained from dissipative dynamics, driving the system to the free-energy minimum. Nonconserved dynamics is used for the height field h,

$$\frac{\partial h}{\partial t} = -\frac{\delta H}{\delta h} + \eta_h(r,t), \tag{3}$$

while, for the density field n, we employ both conservative,

$$\frac{\partial n_h}{\partial t} = \nabla^2\frac{\delta H}{\delta n_h} + \eta_n(r,t), \tag{4}$$

and nonconservative dynamics [in which "∇^2" is replaced with "-1" in Eq. (4)], as in Eq. (3), where η_n and η_h are white-noise terms describing the effects of thermal fluctuations [21,22] at temperature T, with zero mean and

$$\langle \eta_n(\vec{r},t)\eta_n(\vec{r}\,',t')\rangle = 2T\nabla^2\delta(\vec{r}-\vec{r}\,')\delta(t-t') \tag{5}$$

for conservative dynamics and

$$\langle \eta_h(\vec{r},t)\eta_h(\vec{r}\,',t')\rangle = 2T\delta(\vec{r}-\vec{r}\,')\delta(t-t') \tag{6}$$

for nonconservative dynamics.

For the numerical simulations, the coupled Eqs. (3) and (4) are solved numerically in Fourier space [20] with wave vector $\vec{k}$ as a function of time t with time step Δt. A square lattice is used of dimensions $L\Delta x$ and $L\Delta y$ with periodic boundary conditions and mesh sizes $\Delta y \approx \Delta x$. To eliminate small-scale fluctuations of $n(\vec{r}\,)$, $\eta_n(k,t)$ is set to zero for $k > k_{\rm max}$. Typically, the mesh size $\Delta x \approx 0.5$–0.72, time step $\Delta t = 0.2$–0.5, and $k_{\rm max} = 0.5$. Dimensionless units are used in the Hamiltonian with conversion factors for temperature and length $c_{\rm g}/k_{\rm B}$ and 0.353 Å, respectively. In these units, room temperature corresponds to $T \approx 0.004$. In units of the lattice spacing $a_x \sim 4\pi/\sqrt{3}$ of the periodic ground-state configuration [20], the system size corresponds to $L\Delta x/a_x$.

To reach thermal equilibrium, the numerical results described in the following sections were restricted to small system sizes up to $L = 250$ and higher temperatures.

III. DYNAMICS OF HEIGHT FLUCTUATIONS

Height fluctuations in graphene and solid membranes in absence of topological defects can be described by an elasticity theory where the in-plane and out-of-plane deformations are coupled by a nonlinear term [7,8,10]. The combined effect of thermal fluctuations and the nonlinear coupling leads to a flat phase with scale-invariant critical fluctuations, where the mean-square out-of-the plane fluctuations $\langle h_{\rm p}^2\rangle$ increase with system size L as a power law $\langle h_{\rm p}^2\rangle \propto L^{2\xi}$, characterized by the roughening critical exponent ξ. For such membranes, the effective bending stiffness $\kappa(k)$ is renormalized by the thermal fluctuations [9,23], increasing with decreasing wave vector k as $\kappa(k) \sim k^{-\eta}$, and leading to a roughening exponent $\xi = 1 - \eta/2$. Simulations and analytical results for such models give values in the range [24] $\xi = 0.575$–0.66.

The behavior of the mean-squared height displacement, $\langle \Delta h^2\rangle = \langle [h(r,t_0+t) - h(r,t_0)]^2\rangle$, for free-standing graphene in absence of a boundary potential and in-plane strain has been studied recently [12] with the PFC model. The behavior was found to be well described by the dynamic finite-size scaling form [16]

$$\langle \Delta h(t)^2\rangle = L^{2\xi}\Phi(t/L^z), \tag{7}$$

with a roughening exponent $\xi = 0.62(9)$. The dynamic exponent z is constrained to $z = 2(1+\xi)$ from the requirement that the contribution from the center-of-mass diffusion in the long-time limit scales as $\langle \Delta h(t)^2\rangle \sim t/L^2$. This scaling form implies a power-law behavior for the time dependence of height fluctuations, $\langle \Delta h(t)^2\rangle \sim t^\alpha$, with a crossover from an intermediate to long-time regimes with $\alpha = \xi/(1+\xi)$ and $\alpha = 1$, respectively. The subdiffusive behavior at intermediate

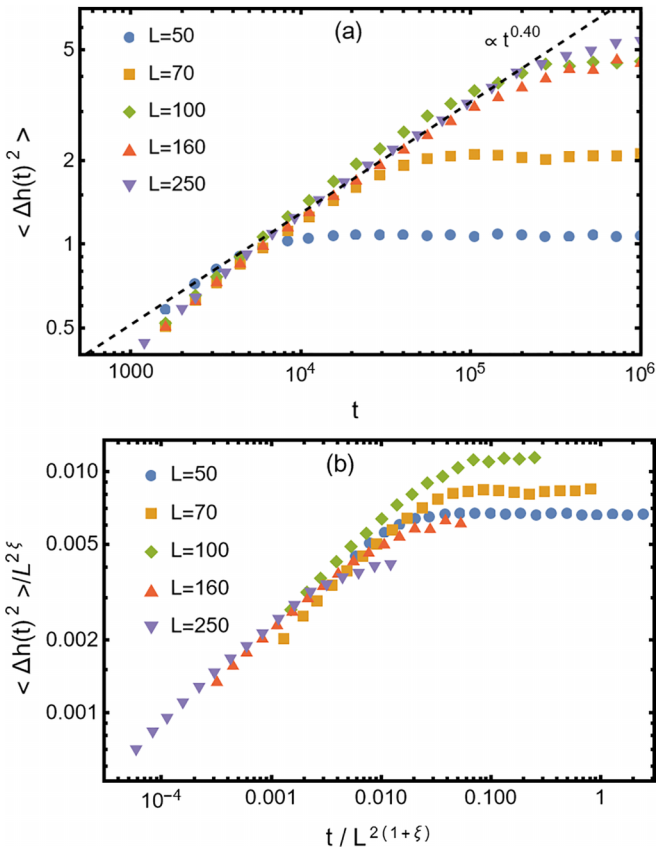

FIG. 1. (a) Mean-square height displacement $\langle \Delta h(t)^2 \rangle$ as a function of time t for different systems sizes L at $T = 0.04$, in presence of a boundary potential with $V_{h0} = 10$. Dotted line is a power-law fit for $L = 250$. (b) Attempt of a scaling plot of the data from Fig. 1 with $\xi = 0.7$. Lack of data collapse indicates that the scaling form of Eq. (7) is not satisfied.

times, $\alpha < 1$, is consistent with measurements of the vertical motion of atoms in free-standing graphene [11] while the long-time behavior, due to the center-of-mass diffusion, has not been observed.

Here, we investigate height fluctuations in graphene membranes in the presence of a boundary potential but still unstrained, where the effects of the potential prevents the center-of-mass diffusion in the long-time limit by favoring $h(\vec{r}\,) = 0$ while $n(\vec{r}\,)$ is still unconstrained. In the experiments, this could be due the interaction of the graphene membrane with the support substrate acting only at the boundaries. Figure 1 shows the finite-size behavior of the mean-square height displacement at the center of the lattice as a function of time for $V_{h0} = 10$ at a pair of opposite boundaries. For the smallest systems, a crossover from an intermediate to a saturation regime is clear seen. For the largest system $L = 250$, the behavior at intermediate times is still subdiffusive with $\alpha \approx 0.4$. Nevertheless, as shown in Fig. 1, data collapse on a single curve is not observed adjusting the value of ξ. This indicates that the simple scaling form of Eq. (7) in terms of a scaling function of a single variable t/L^z is not satisfied for all times. It suggests that another length scale besides the system size L should be taken into account. In fact, in the presence of the boundary potential $V_h(\vec{r}\,)$ in Eq. (1), an additional length scale L_b is set by the corresponding energy contribution of the order of kT. As a result, the scaling function in Eq. (7) should also depend on an additional variable L/L_b, which is size dependent. Surprisingly, however, α is comparable to the value obtained without the boundary potential, $\alpha = \xi/(1+\xi) \approx 0.38$. This result can still be understood from the scaling behavior of Eq. (7) when restricted to times below the crossover to the saturation regime for large systems. In this case, the contribution to $\langle \Delta h(t)^2 \rangle$ from the center-of-mass diffusion, $\approx t/L^2$, is limited by the out-of-plane fluctuations at saturation $L^{2\xi}$, corresponding to a relaxation time [16] $\tau \propto L^z$ with dynamic exponent $z = 2(\xi + 1)$ and consequently the same diffusion exponent $\alpha = 2\xi/z = \xi/(\xi + 1)$.

Therefore, even in the presence of pinned boundaries, the height displacement fluctuations of unstrained graphene display subdiffusive behavior at intermediate times, as observed in the experiments [11] in free-standing graphene. However, in the long-time limit a saturation regime appears, which could in principle be verified in experiments with controlled boundary potentials.

IV. MIRROR-BUCKLING FLUCTUATIONS AND PHASE TRANSITION

In the presence of an externally applied in-plane compression, thermally induced fluctuations of large amplitude have been observed in molecular-dynamics simulations of graphene membranes [11,17], where the height configurations spontaneously invert their curvature as a function of time with sharp and well-separated bounces. Since the origin and the effects of such mirror-buckling fluctuations on the subdiffusive behavior of the height displacement found in experiments [11] by scanning tunneling microscopy are still not fully understood [12,25], investigating their temperature dependence may provide useful information. Here we first demonstrate that this behavior can also be reproduced with the PFC model of Eq. (1) under external compression and then determine the effects of varying the temperature in equilibrium.

To study the system under compression and pinned boundaries we allow for nonzero boundary potentials for both $n(\vec{r}\,)$ and $h(\vec{r}\,)$ in the Hamiltonian. To pin the boundaries, $V_h(\vec{r}\,)$ was initially set to zero in the central region of the simulation cell and $V_h(\vec{r}\,) = V_{h0} = 1$ in the region 10 lattice sites from the edges. To avoid numerical anomalies, $V_h(\vec{r}\,)$ was then smoothed in Fourier space by $e^{-k^2/2}$. A similar process was used for $V_n(\vec{r}\,)$ except that, near the edges, $V_n(\vec{r}\,)$ was set to a one mode approximation for n, i.e., $V_n = V_{h0} \sum_j e^{i\epsilon \vec{q}_j \cdot \vec{R}}$, where $\vec{q}_1 = (-\sqrt{3}, -1)/2$, $\vec{q}_2 = (0, 1)$, and $\vec{q}_3 = (\sqrt{3}, -1)/2$. The parameter ϵ is used to control the average strain, which is given approximately by $(1 - \epsilon)/\epsilon$. V_n and V_h were fixed throughout the simulation. To mimic prior studies [11,17,20], the density was initially set to $n = -\phi(\sum_j e^{i\vec{q}_j \cdot \vec{r}} + \text{c.c.})$, where ϕ is the amplitude that minimizes the ground-state energy and c.c. is the complex conjugate.

Figure 2 shows the behavior of the spatially averaged height,

$$\bar{h}(t) = \sum_{\vec{r}} h(\vec{r}, t)/L^2, \tag{8}$$

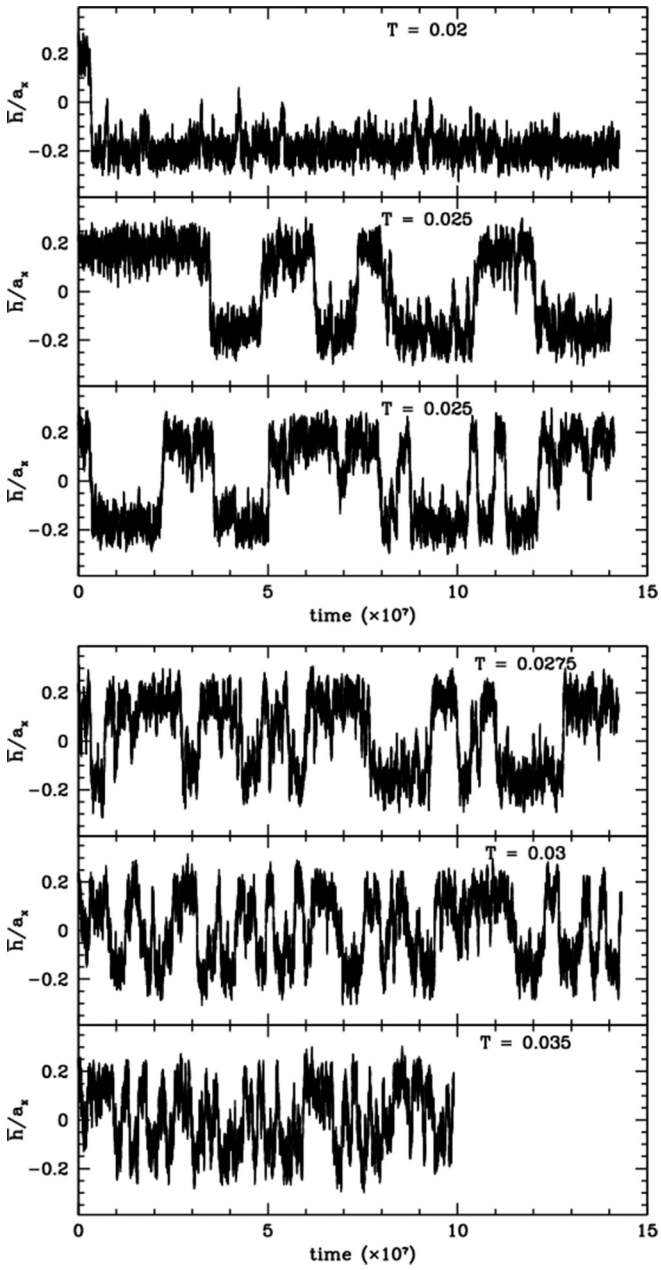

FIG. 2. Time dependence of the average height $\bar{h}$ for different temperatures for the graphene membrane under compressive strain of 1.8% and system size $L = 160$. The two figures for $T = 0.025$ correspond to different starting configurations

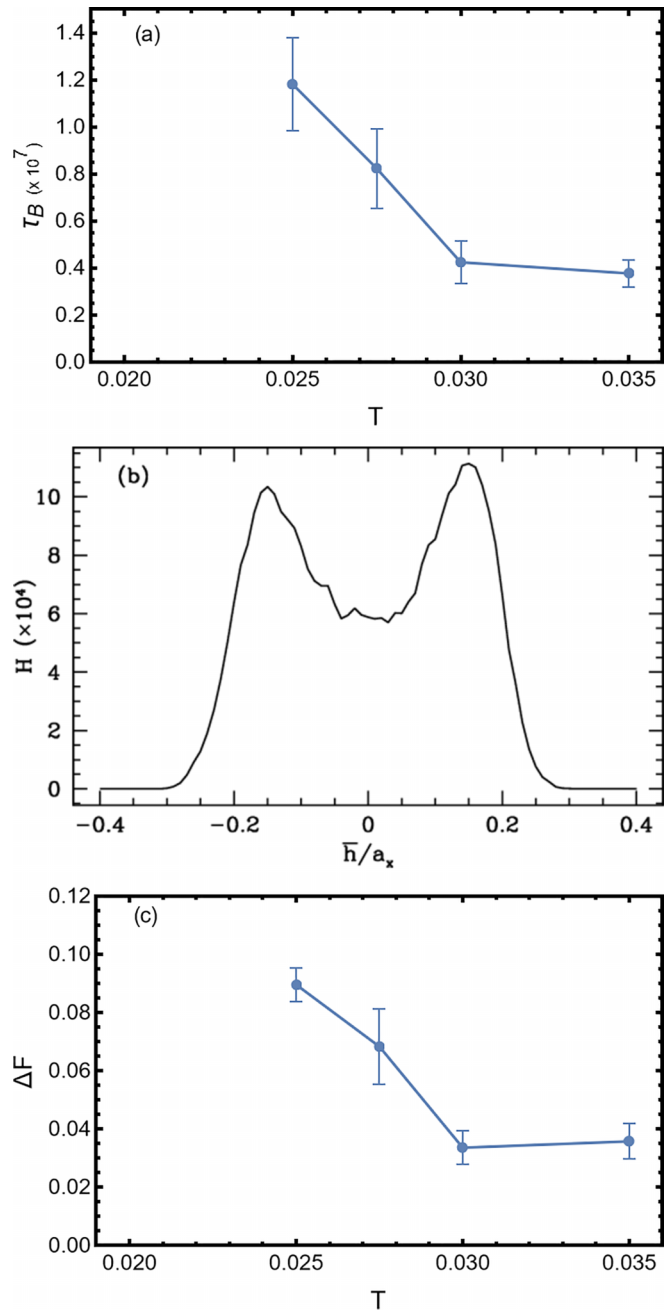

FIG. 3. (a) Average time period between buckling fluctuations from Fig. 2 as a function of temperature. (b) Probability distribution of the average height $\bar{h}$ at $T = 0.03$. (c) Temperature dependence of the free-energy barrier ΔF for buckling fluctuations.

as a function of time, for different temperatures with $\epsilon = 1.018\,031\,58$. In addition to fluctuations of small amplitude at short timescales, there are sharp and large fluctuations with height inversion from values above to below the pinned boundaries with $h = 0$. Such spontaneous height inversions at the intermediate temperatures, $T = 0.025$ and 0.0275, are very similar to those observed previously in molecular-dynamics simulations of atomistic models of graphene [11,17] as a local curvature inversion of the height at the central region. Here we find that the average time τ_B between height inversions increases quickly with decreasing temperature as shown in Fig. 3(a), becoming larger than the available simulation time below $T_c \approx 0.025$. One expects that τ_B is determined by the free-energy barrier ΔF between buckled configurations with opposite heights. We can obtain ΔF as

$$\Delta F = -T \ln (p_m/p_M), \tag{9}$$

for each temperature from the probability distribution $p(\bar{h})$, which displays a double peak structure like the one in Fig. 3(b) with minimum p_m and maximum p_M. As for τ_B, the free-energy barrier also increases quickly with decreasing temperature as shown in Fig. 3(c), but below T_c it is too large to lead to a double-peak structure in the height probability

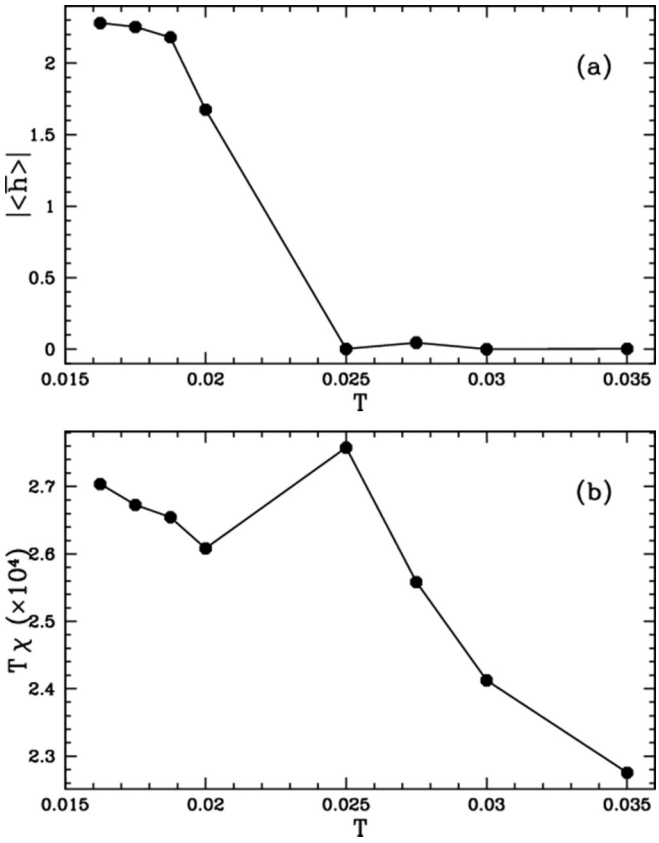

FIG. 4. (a) Time-averaged height $\langle \bar{h} \rangle$ as a function of temperature. (b) Temperature dependence of the height susceptibility χ.

distribution. As a result, the increase in τ_B is not just the effect of decreasing temperature, as would be expected if τ_B is given by the Kramers equation $\tau_B \propto e^{U/k_B T}$, where U is an approximately constant energy barrier. Thus, using such an equation to estimate the energy barrier for mirror buckling as employed in the molecular-dynamics study [17], can lead to inconsistent results.

To further characterize the temperature dependence of the buckling fluctuations, we show in Fig. 4(b) the behavior of the time-averaged height $\langle \bar{h} \rangle$ and corresponding susceptibility

$$\chi = L^2 \left(\langle \bar{h}^2 \rangle - \langle \bar{h} \rangle^2 \right) / T. \tag{10}$$

The susceptibility displays a maximum at approximately the same temperature T_c where the average height becomes significantly different from zero and τ_B is larger. The behavior described above for $\bar{h}$ and χ signals a buckling phase transition at T_c, below which the inversion height symmetry of the model of Eq. (1) is spontaneously broken and the graphene membrane is buckled with $\langle \bar{h} \rangle \neq 0$, while above T_c it is flat with $\langle \bar{h} \rangle = 0$. In the thermodynamic limit, χ should diverge if the transition is continuous. As shown in Fig. 5, the transition temperature depends on the compression. It vanishes at the critical compression corresponding to the zero-temperature long-wavelength elastic instability of the graphene membrane [18], which depends on the system size. For the PFC model, it can be estimated approximately as [20] $Q^2\kappa/9B_x\phi^2$, where ϕ is the amplitude of phase field $n(\vec{r}\,)$ and $Q = 2\pi/L$ is the

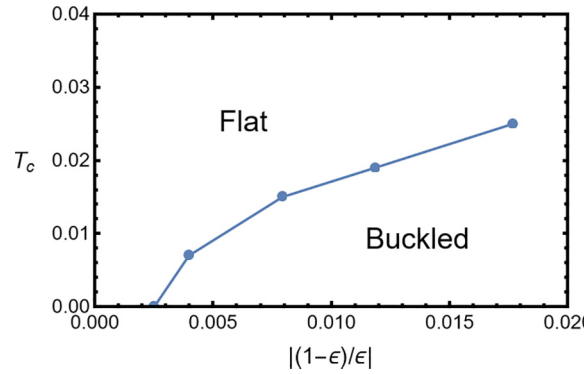

FIG. 5. Critical temperature of the buckling transition as a function of compressive strain parametrized by ϵ.

smallest wave vector. At finite temperatures, the buckling threshold increases due to an enhancement of the effective bending stiffness $\kappa(k)$ by long-wavelength thermal fluctuations [9]. Figure 6 illustrates two typical height configurations just above and below the transition while Fig. 7 shows the same data combining height and density field configurations.

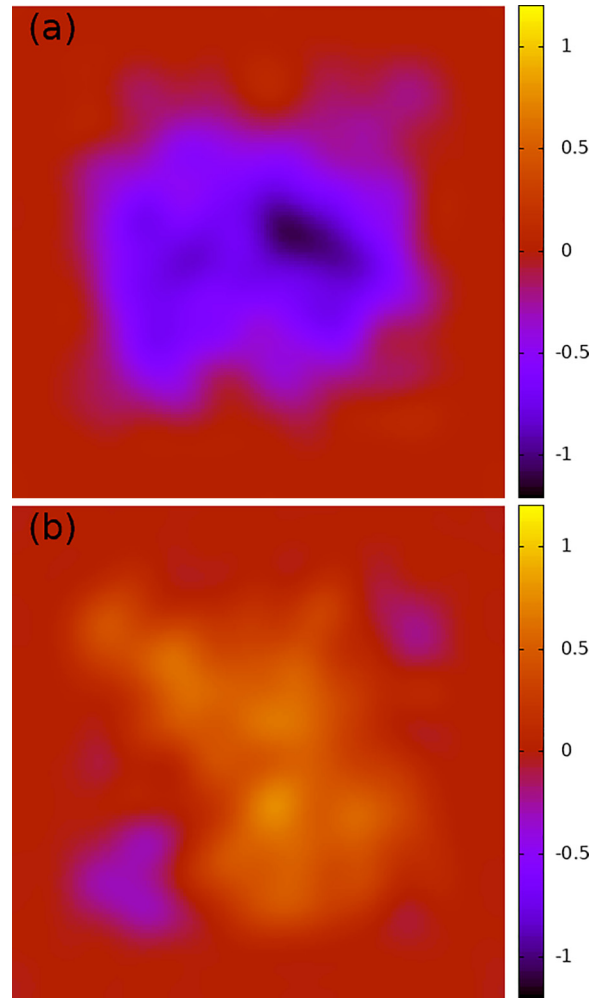

FIG. 6. Sample height configurations for just below (a) $T = 0.02$ and above (b) $T = 0.03$ the buckling transition.

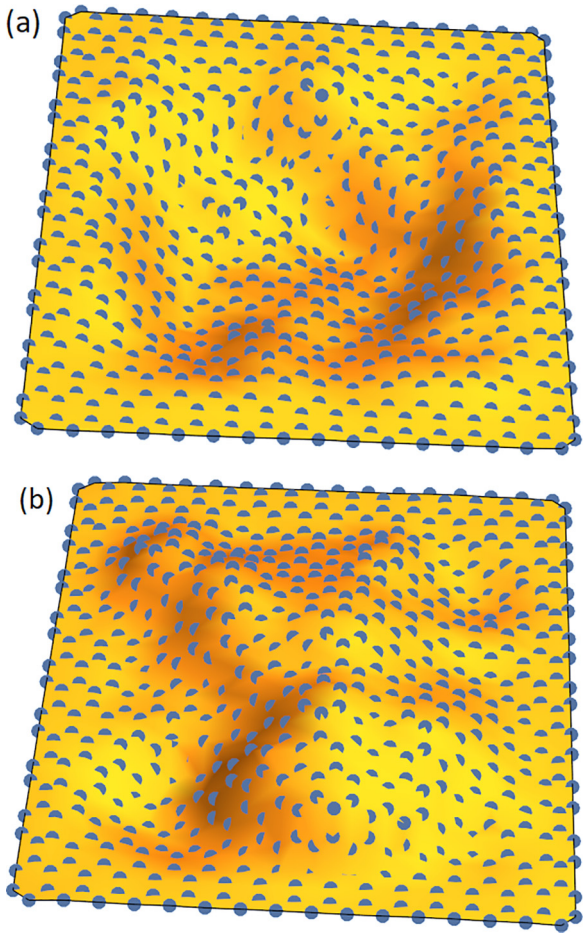

FIG. 7. Same as Fig. 6 but combining height and density field configurations. (a) $T = 0.02$ and (b) $T = 0.03$. Filled circles represent the density field maxima.

Recently, the buckling transition in thermalized membranes with clamped boundaries and driven by compressive strain has been studied analytically by renormalization-group methods [18], revealing universal critical scaling exponents and nonlinear height response that should be independent of the microscopic details of the model. Our results from the PFC model of Eq. (1) with pinned boundaries and fixed compression provide evidence of such transition driven by thermal fluctuations. It also indicates that the well time separated and sharp mirror-buckling fluctuations in Fig. 2 are a signature of the nearby thermal buckling transition.

V. NONLINEAR HEIGHT RESPONSE NEAR THE BUCKLING TRANSITION

The proximity to the buckling transition presented in the previous section has also important effects on the height response to an external force applied perpendicularly to the membrane [18]. Such force-displacement relations have recently been measured in experiments on graphene membranes with clamped boundaries [5] under an applied electric field.

To study the height response to an external transverse force f, an additional term is included in the effective Hamiltonian of Eq. (1) describing the linear coupling of the height to the force, $-f \int d^2\vec{r}\, h(\vec{r}\,)$. The relation between the external force and the average height has recently been obtained from a renormalization-group study of compressed membranes [18]. In our case, where the compression is fixed and the temperature is the tuning parameter, this relation can be rewritten as [18]

$$f = c_1 \Delta T \langle \bar{h} \rangle^{3-1/\beta} + c_2 \langle \bar{h} \rangle^3, \tag{11}$$

where β is the critical exponent describing the vanishing of the average height near the transition, $\langle \bar{h} \rangle \propto \Delta T^{\beta}$, in absence of the force, with $\Delta T = T - T_c$. The critical temperature T_c and the constants c_1 and c_2 depend on the system size in addition to the elastic constants, a peculiar feature of the buckling transition. Here, we will consider a fixed system size with $L = 160$. A notable result from this renormalization-group study is the value of critical exponent for membranes with clamped boundaries, $\beta = 0.718$, which leads to a significant difference of the exponent $3 - 1/\beta = 1.607$ of the first term in this equation from the expected linear term from mean-field theory, for which $\beta = 1/2$. At the transition, the height response behaves as a power law, $\langle \bar{h} \rangle \propto f^{1/\delta}$, with the critical exponent $\delta = 3$.

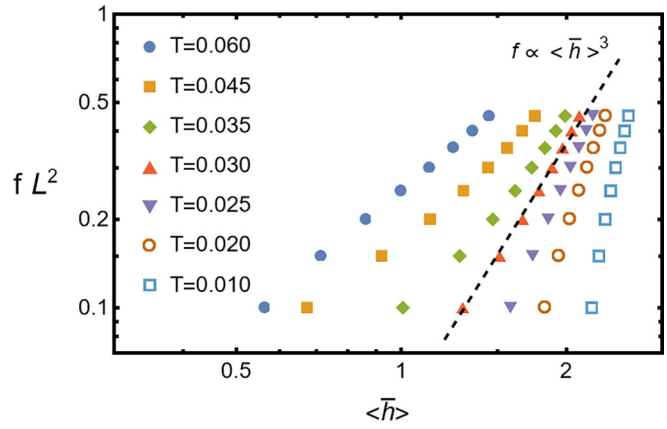

FIG. 8. Height response behavior under externally applied force f for different temperatures T near the buckling transition of Fig. 4. The dashed line corresponds to the power-law behavior with exponent 3 expected at the transition.

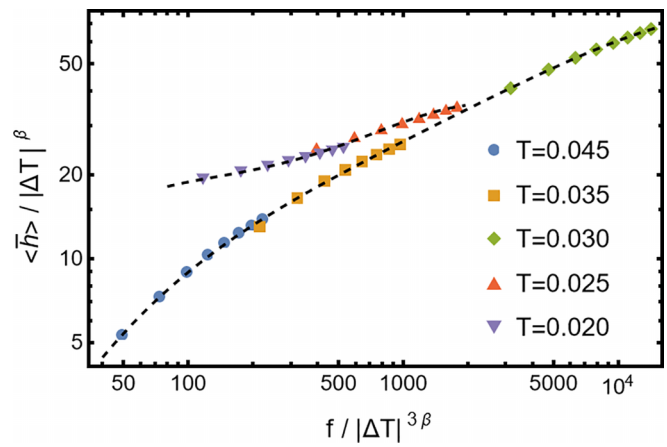

FIG. 9. Scaling plot of the height response near the buckling transition with $\Delta T = T - T_c$ for $T_c = 0.029$ and $\beta = 0.5$.

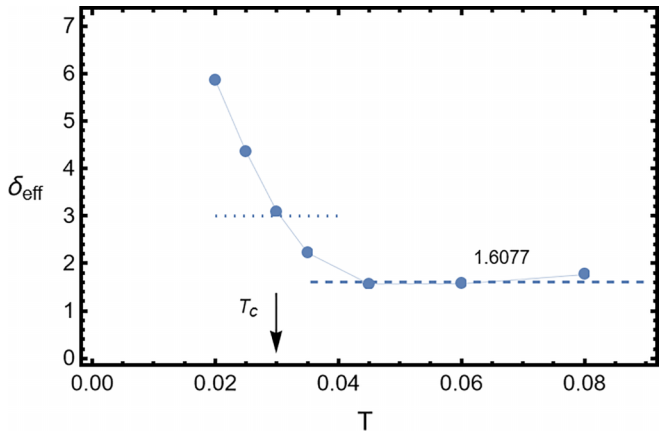

FIG. 10. Effective exponent δ_{eff} from a power-law fit, $f \propto \langle \bar{h} \rangle^{\delta_{\text{eff}}}$, as a function of temperature. The dashed line corresponds to the exponent $3 - 1/\beta = 1.607$ predicted by the renormalization-group calculations of Ref. [18].

Near the transition, the height response should also satisfy the scaling form

$$\langle \bar{h} \rangle = \Delta T^{\beta} \Phi^{\pm}(f/\Delta T^{3\beta}), \tag{12}$$

where $\pm$ correspond to temperatures above and below T_c.

Figure 8 shows behavior of the force as a function of the height near the transition, for the PFC model under compression and pinned boundaries presented in the previous section. The dashed line corresponds to the power-law behavior $f \propto h^{\delta}$ with exponent $\delta = 3$ expected at the transition, which is consistent with a critical temperature $T_c \approx 0.03$. In Fig. 9, we show a scaling plot of the height response according to Eq. (12), obtained by adjusting the parameters T_c and β. The data collapse onto two different curves, supporting the scaling theory and providing an estimate of β. Although a reasonable data collapse is obtained for $\beta = 0.5(2)$, the large error bar and the neglect of finite-size effects does not allow us to rule out the mean-field behavior from this scaling plot. On the hand, away from the transition, finite-size effects are expected to be negligible as the correlation length becomes smaller than the system size. Then, defining an effective critical exponent δ_{eff} from a power-law fit $f \propto \langle \bar{h} \rangle^{\delta_{\text{eff}}}$ for data at different temperatures, we can follow the crossover from its value equals three at the transition to a smaller value at higher temperatures as ΔT increases, when the first term in Eq. (11) dominates over the second term for small forces. As shown in Fig. 10, it approaches an exponent consistent with the value $3 - 1/\beta = 1.607$ predicted by the renormalization-group calculations. As argued in Ref. [18] this critical exponent describes the anomalous nonlinear response observed in experiments on graphene membranes with clamped boundaries [5].

VI. SUMMARY AND CONCLUSIONS

Using the PFC model with out-of-plane deformations introduced previously [20] and extended to include the effects of boundary potentials, we have investigated the effects of thermal fluctuations in graphene membranes with pinned boundaries. It is found that, at sufficiently long times, the linear diffusive behavior of height fluctuations observed recently with the same model for systems with free boundaries [12] becomes a saturation regime in presence of pinned boundaries, while at intermediate times the behavior remains subdiffusive, as observed experimentally [11]. Under compression with pinned boundaries, we find mirror buckling fluctuations similar to the behavior observed by molecular-dynamics simulations of atomistic models [11,17], which has been argued to also be responsible for the non-Gaussian velocity distribution observed in the experiments [11]. Interestingly, we find that the average time between fluctuations diverges below a critical temperature corresponding to a thermal buckling transition. Below the transition, the graphene membrane is buckled while above the transition it is flat but with small fluctuations. Recently, this transition has been studied analytically by renormalization-group methods [18], revealing critical exponents and nonlinear height response depending in a nontrivial way on the boundary constraints at constant strain or stress. In addition to providing numerical evidence of such transition driven by thermal fluctuations, our results also indicate that the well time separated and sharp mirror-buckling fluctuations are a signature of the nearby thermal buckling transition, thereby suggesting a possible origin of the anomalous velocity distribution observed experimentally [11]. The proximity to this buckling transition also has important effects on the height response to an external force applied perpendicularly to the membrane, as measured in experiments on graphene membranes with clamped boundaries [5]. We find a nonlinear force-displacement relation with an exponent consistent with the value $3 - 1/\beta = 1.607$ as predicted by renormalization-group calculations [18] and observed in these experiments as an anomalous height response. Our results demonstrate the importance of boundary constraints in the effects of thermal fluctuations on the long-wavelength behavior and buckling of graphene membranes [18,19] and show that the PFC model with out-of-plane deformations can provide a useful framework for further investigations.

ACKNOWLEDGMENTS

E.G. was supported by the National Council for Scientific and Technological Development-CNPq and computer facilities from CENAPAD-SP. K.R.E. would like to acknowledge support of the National Science Foundation (NSF) under Grant No. DMR-2006456 and Oakland University Technology Services high performance computing facility (Matilda). T.A-N. has been supported in part by the Academy of Finland through its QTF Center of Excellence program Grant No. 312298.

[1] P. G. Steeneken, R. J. Dolleman, D. Davidovikj, F. Alijani, and H. S. Van Der Zant, Dynamics of 2D material membranes, 2D Mater. **8**, 042001 (2021).

[2] P. M. Thibado, P. Kumar, S. Singh, M. Ruiz-Garcia, A. Lasanta, and L. L. Bonilla, Fluctuation-induced current from freestanding graphene, Phys. Rev. E **102**, 042101 (2020).

[3] M. Neek-Amal, P. Xu, J. Schoelz, M. Ackerman, S. Barber, P. Thibado, A. Sadeghi, and F. Peeters, Thermal mirror buckling in freestanding graphene locally controlled by scanning tunnelling microscopy, Nat. Commun. **5**, 4962 (2014).

[4] J. S. Bunch, A. M. van derZande, S. S. Verbridge, I. W. Frank, D. M. Tanenbaum, J. M. Parpia, H. G. Craighead, and P. L. McEuen, Electromechanical resonators from graphene sheets, Science **315**, 490 (2007).

[5] I. R. Storch, R. De Alba, V. P. Adiga, T. S. Abhilash, R. A. Barton, H. G. Craighead, J. M. Parpia, and P. L. McEuen, Young's modulus and thermal expansion of tensioned graphene membranes, Phys. Rev. B **98**, 085408 (2018).

[6] J. C. Meyer, A. K. Geim, M. I. Katsnelson, K. S. Novoselov, T. J. Booth, and S. Roth, The structure of suspended graphene sheets, Nature (London) **446**, 60 (2007).

[7] A. Fasolino, J. Los, and M. I. Katsnelson, Intrinsic ripples in graphene, Nat. Mater. **6**, 858 (2007).

[8] J. H. Los, M. I. Katsnelson, O. Yazyev, K. V. Zakharchenko, and A. Fasolino, Scaling properties of flexible membranes from atomistic simulations: Application to graphene, Phys. Rev. B **80**, 121405(R) (2009).

[9] D. Nelson and L. Peliti, Fluctuations in membranes with crystalline and hexatic order, J. Phys. (Paris) **48**, 1085 (1987).

[10] D. Nelson, T. Piran, and S. Weinberg, *Statistical Mechanics of Membranes and Surfaces* (World Scientific, Singapore, 2004).

[11] M. L. Ackerman, P. Kumar, M. Neek-Amal, P. M. Thibado, F. M. Peeters, and S. Singh, Anomalous Dynamical Behavior of Freestanding Graphene Membranes, Phys. Rev. Lett. **117**, 126801 (2016).

[12] E. Granato, M. Greb, K. R. Elder, S. Ying, and T. Ala-Nissila, Dynamic scaling of out-of-plane fluctuations in freestanding graphene, Phys. Rev. B **105**, L201409 (2022).

[13] M. Smirman, D. Taha, A. K. Singh, Z.-H. Huang, and K. R. Elder, Influence of misorientation on graphene Moiré patterns, Phys. Rev. B **95**, 085407 (2017).

[14] P. Hirvonen, Z. Fan, M. M. Ervasti, H. Ari, E. K.R., and T. Ala-Nissila, Energetics and structure of grain boundary triple junctions in graphene, Sci. Rep. **7**, 4754 (2017).

[15] P. Hirvonen, M. M. Ervasti, Z. Fan, M. Jalalvand, M. Seymour, S. M. V. Allaei, N. Provatas, A. Harju, K. R. Elder, and T. Ala-Nissila, Multiscale modeling of polycrystalline graphene: A comparison of structure and defect energies of realistic samples from phase field crystal models, Phys. Rev. B **94**, 035414 (2016).

[16] K.-I. Mizuochi, H. Nakanishi, and T. Sakaue, Dynamical scaling of polymerized membranes, Europhys. Lett. **107**, 38003 (2014).

[17] J. M. Mangum, F. Harerimana, M. N. Gikunda, and P. M. Thibado, Mechanisms of spontaneous curvature inversion in compressed graphene ripples for energy harvesting applications via molecular dynamics simulations, Membranes (Basel, Switz.) **11**, 516 (2021).

[18] S. Shankar and D. R. Nelson, Thermalized buckling of isotropically compressed thin sheets, Phys. Rev. E **104**, 054141 (2021).

[19] A. Morshedifard, M. Ruiz-García, M. J. A. Qomi, and A. Košmrlj, Buckling of thermalized elastic sheets, J. Mech. Phys. Solids **149**, 104296 (2021).

[20] K. R. Elder, C. V. Achim, V. Heinonen, E. Granato, S. C. Ying, and T. Ala-Nissila, Modeling buckling and topological defects in stacked two-dimensional layers of graphene and hexagonal boron nitride, Phys. Rev. Mater. **5**, 034004 (2021).

[21] J. A. P. Ramos, E. Granato, C. V. Achim, S. C. Ying, K. R. Elder, and T. Ala-Nissila, Thermal fluctuations and phase diagrams of the phase-field crystal model with pinning, Phys. Rev. E **78**, 031109 (2008).

[22] J. A. P. Ramos, E. Granato, S. C. Ying, C. V. Achim, K. R. Elder, and T. Ala-Nissila, Dynamical transitions and sliding friction of the phase-field-crystal model with pinning, Phys. Rev. E **81**, 011121 (2010).

[23] P. Chaikin and T. Lubensky, *Principles of Condensed Matter Physics* (Cambridge University Press, Cambridge, 1995).

[24] A. Tröster, High-precision Fourier Monte Carlo simulation of crystalline membranes, Phys. Rev. B **87**, 104112 (2013).

[25] Y. Kai, W. Xu, B. Zheng, N. Yang, K. Zhang, and P. Thibado, Origin of non-Gaussian velocity distribution found in freestanding graphene membranes, Complexity **2019**, 1 (2019).